Optica Applicata, Vol. XXX, No. 2–3, 2000

Optimized CGH-based pattern recognizer

LESZEK R. JAROSZEWICZ

Institute of Applied Physics, Military University of Technology, ul. Kaliskiego 2, 00-908 Warszawa, Poland.

KRZYSZTOF A. CYRAN, TOMASZ PODESZWA

Institute of Computer Science, Silesian Technical University, ul. Akademicka 16, 44-100 Gliwice, Poland.

A pattern recognition system with the computer-generated hologram used as feature extractor, useful in many applications, is considered in the paper. The method of optimization of such extractors, based on modified evolutionary algorithm with elements of rough set theory used to define a proper objectve function, is also presented. The theoretical investigations are supported with experimental works for two different applications of optimized system. The applications are examples of a wide area of pattern recognition problems where proper characteristic features are not easy to determine. The results obtained confirm the enhancement of system optimized with proposed method compared to systems with standard computer-generated hologram.

1. Introduction

The rapid development of hybrid, optical-digital pattern recognition systems can be observed in the last decades [1]–[3]. In such systems, usually the optical part implements the fast feature extraction, while digital part performs the classification of features. An example of this strategy is a hybrid system in which the lens and a ring-wedge detector (RWD) have been used as the feature extractor [4]. The classification of features extracted by it was done using artificial neural network (ANN).

However, the utilization of RWD in many applications is very questionable, due to its poor flexibility [3]. Therefore, a computer-generated hologram (CGH) has been suggested as a cheaper and more flexible element compared to RWD [5]. Although this suggestion does not consider directly the problem of classification, the promising classification results obtained with RWD [4] are obviously valid also for CGH-based systems. The CGH-based feature extractor is also suitable for use with optical implementations of neural networks. This technology, dynamically growing nowadays, opens up the gate for extremely fast, real time applications [6]. Moreover, easy modification of the CGH size makes it possible to optimize such feature extractor for a given recognition task. This was the motivation the design of an optimized CGH-based pattern recognizer.

The general idea and first experiment concerning the original method of CGH optimization were reported in [7]. A detailed optical-arrangement of the system used

for this early experiment has been reported in [8], whereas the paper [9] focused on aspects of rough sets applied to this optimization method. The latter paper has shown that one of the coefficients defined by rough set theory (RST) could be used as a good objective function for stochastic evolutionary search in the space of possible solutions. The development of the proposed method (concerning especially the problem of constraints in evolutionary optimizing search) has been observed since then. Also the range of experiments has grown. The CGH-based system optimized with the present method seems to be useful in many pattern recognition problems.

The purpose of this paper is to summarize previously partially reported efforts and results by presenting the optimized CGH-based recognizer, as well as to give current experimental results. The following section based on the foundations of pattern recognition systems provides the description of hybrid optical-digital pattern recognizers. It also emphasizes and explains the advantages of computer-generated hologram in comparison with ring-wedge detectors. The section ends with the description of software simulated CGH-ANN system and its properties. In the next section, the general explanation of the optimization method, as well as the discussion on dealing with the constraints in evolutionary algorithms, are provided. Finally, the experimental work concerning two different applications using optimized system is presented.

2. CGH-based pattern recognition system

Pattern recognition is the special, and at the same time, very important case of general recognition problem. The recognition can be expressed as a concatenation of two subsequent operations. The first is the extraction of characteristic features from input data (from image space, when image pattern recognition is considered). The second operation is a classification of previously extracted characteristic features [10]. By recognition, the capability of classification is often meant. In this way recognition problems are formalized as feature extraction and classification containing additional "unknown" class, indicating the situation when none of normal classes is recognized with required certainty [11].

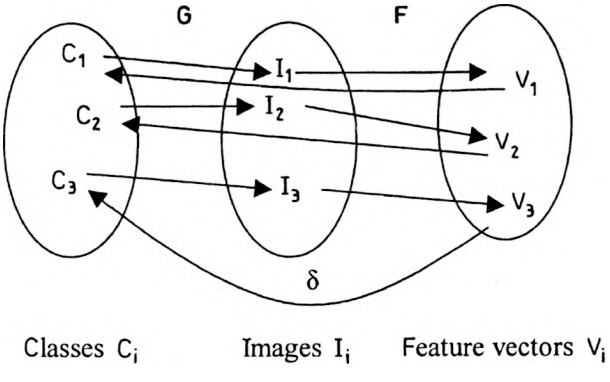

Fig. 1. Mappings of pattern recognition problem [10].

Mappings that occur in pattern recognition are shown in Fig. 1. Objects C_i from class space C are transformed by mapping G into image space I consisting of images I_i. Next mapping F transforms objects from image space into feature space V. Theoretically, the recognition of images from space I can be expressed without considering mapping F as looking for mapping G^{-1}. However, the size of data describing objects in space I is so large that obtaining direct mapping G^{-1} is very difficult. Therefore, the indirect approach is applied. First, the mapping F is found. It transforms objects from space I into objects from space V with reduced dimensionality.

It is important to assure that objects from space V after this transformation preserve the information required for classification. The purpose of mapping δ (representing the classification) is to transform objects from V into objects from C. It is evident that

$$\delta = (G \circ F)^{-1}. \tag{1}$$

The system implementing this idea and recognizing image as belonging to the class C_i according to

$$C_i = \delta(F(I_i)) \tag{2}$$

is presented in Fig. 2.

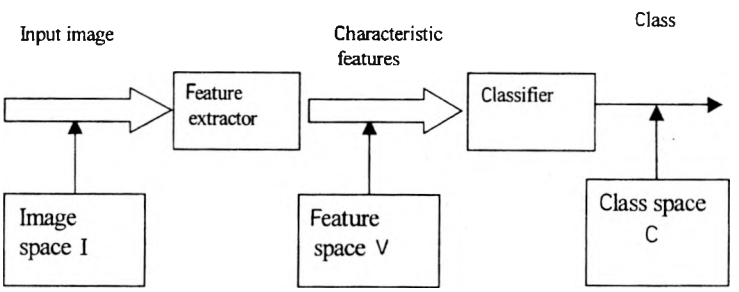

Fig. 2. Pattern recognizer scheme [9].

Equation (2) indicates that, for good overall operation of the system, the proper definition of the mapping $F : I \rightarrow V$ is required. However, it is not easy to find such mapping that reduces dimensionality of the space and at the same time does not lose information essential for classification. Mappings that utilize Fourier transformation in the first stage of feature extraction are very promising. One of them uses ring-wedge detector extracting features from frequency domain images. Hence, some technical applications of this approach are described below.

2.1. Ring-wedge detector as feature extractor

The ring-wedge detector is a circular element consisting of special detection regions in the form of rings RING(i) and wedges WEDGE(i), as shown schematically in Fig. 3 [1]. Ring-wedge detector is placed in Fourier plane of the optical system.

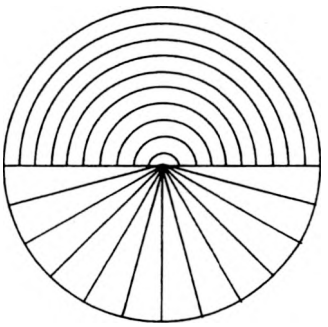

Fig. 3. Scheme of ring-wedge detector [1].

Therefore, the intensity of light on the surface of RWD is the intensity of the Fourier transform $F(u, v)$ of input image function $f(x, y)$. Each of RWD regions performs two operations. The first operation is an integration of the intensity of light passing through the given region. Let us denote the integrated light intensity of ring RING(i) by R_i and integrated light intensity of the wedge WEDGE(i) by W_i. Then

$$R_i = \iint_{u,v \in \mathrm{RING}(i)} F^2(u, v)\,\mathrm{d}u\,\mathrm{d}v \tag{3}$$

and

$$W_i = \iint_{u,v \in \mathrm{WEDGE}(i)} F^2(u, v)\,\mathrm{d}u\,\mathrm{d}v. \tag{4}$$

The important feature is that intensity R_i is shift and rotation invariant, as well as intensity W_i is shift and scale invariant [1].

The second operation performed by RWD is a conversion of the integrated light intensities W_i and R_1 into electronic signals. This is done by planar photodetectors that cover rings and wedges of the RWD element.

After both operations (performed in parallel) on the output of RWD a vector of shift, rotation and scale invariant characteristic features is available as a set of electric signals. Therefore, such a device can be easily applied to recognize the same patterns shifted, rotated or resized as belonging to the same class [4], [12].

2.2. Hybrid optical-digital system

Despite the fact that features obtained from RWD are invariant with respect to typical transformations of input image, the utilization of RWDs is very difficult in applications. This is due to fixed size of rings and wedges in RWD. This fixed size is the reason of a very poor flexibility of RWD-based feature extractors. The second disadvantage is connected with the high cost of RWD elements. Both of them can be overcome with the use of computer-generated hologram [5]. The main idea of a system with CGH was to separate in space (but not in time) the two operations performed by RWD. The operation of the hybrid CGH-based pattern recognizer is shown in Fig. 4.

The CGH itself performs only light integration and diffracts integrated light beams into different angles and orientations. A conversion to electric signal is

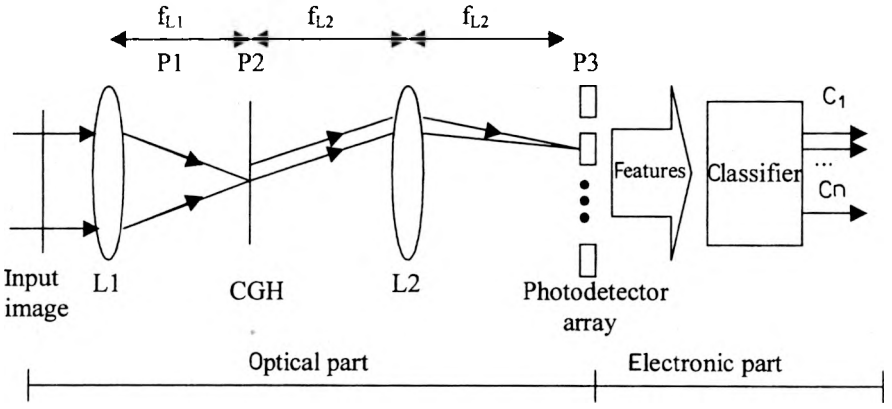

Fig. 4. Hybrid CGH-based pattern recognition system [7].

done by cheap quasi-point photodetectors placed in plane P3 (Fig. 4). Moreover, the CGH system can be simulated and processed in the digital equipment. Digital processing is discrete. Therefore, continuous variables (like integrated light intensities) have to be represented as discrete variables. This always leads to the loss of information. However, the way of sampling should minimize this loss.

Let us take into consideration independent, scalar continuous variable x such that $X_1 \leqslant x \leqslant X_2$. This continuum range $X = (X_1, X_2)$ has to be replaced by a set of points by dividing the range X into $N-1$ elements Δx_n. These elements define the vector $\mathbf{x} = [x_1, x_2, \ldots, x_N]$ of the size N such that [13]

$$x_n = X_1 + \sum_{i=1}^{n-1} \Delta x_i. \tag{5}$$

The function $f(x)$ of continuous variable x can be represented by a vector $\mathbf{f} = [f_1, f_2, \ldots, f_N]$ such that

$$f_n = f(x_n). \tag{6}$$

The function f can be approximated using the vector $\mathbf{f}$ in any point by interpolation. Let us denote by x' a continuous variable such that

$$x_n \leqslant x' \leqslant x_{n+1}. \tag{7}$$

Then $f^{(*)}$ is the approximation of the continuous function f if

$$f^{(*)} = \varepsilon f_{n+1} + (1-\varepsilon) f_n \tag{8}$$

where

$$\varepsilon = \frac{x' - x_n}{x_{n+1} - x_n}. \tag{9}$$

These considerations can be extended to two-dimensional independent variables and two-dimensional functions. Let us divide the domain of the continuous image function $f(x, y)$ into M intervals of the length Δx in x direction and into N intervals

of the length Δy in y direction. Then matrix $\mathbf{f} = f(m\Delta x, n\Delta y)$ for $m = 1,\ldots,M$, $n = 1,\ldots,N$ is a sampled image of the continuous image $f(x,y)$. Sampled image with amplitude represented by discrete numbers (process of quantization) is a discrete image.

The new image $\mathbf{F}$ is a discrete Fourier transform of the image $\mathbf{f}$ if [14]

$$\mathbf{F} = \boldsymbol{\Phi}_{MM}\,\mathbf{f}\,\boldsymbol{\Phi}_{NN} \tag{10}$$

where matrix of the Fourier transform $\boldsymbol{\Phi}_{JJ}$ of the size $J \times J$ is given by

$$\Phi_{JJ}(k,l) = \frac{1}{J}\exp\left(-i\frac{2\pi}{J}kl\right), \qquad k,l = 0,\ 1,\ldots,J-1. \tag{11}$$

Therefore

$$F(u,v) = \frac{1}{MN}\sum_{m=0}^{M-1}\sum_{n=0}^{N-1} f(m,n)\exp\left[-i2\pi\left(\frac{mu}{M}+\frac{nv}{N}\right)\right] \tag{12}$$

where: $u = 0,\ 1,\ldots,M-1$, $v = 0,\ 1,\ldots,N-1$. Function $k:\mathrm{R}^4 \to \mathrm{C}$ is a kernel of the Fourier transform if

$$k = \exp\left[-i2\pi\left(\frac{mu}{M}+\frac{nv}{N}\right)\right]. \tag{13}$$

Matrix of the discrete inverse Fourier transform $\boldsymbol{\Phi}_{JJ}^{-1}$ is then defined by

$$\Phi_{JJ}^{-1}(k,l) = \exp\left(i\frac{2\pi}{J}kl\right), \quad k,l = 0,\ 1,\ldots,J-1. \tag{14}$$

Therefore

$$f(m,n) = \sum_{u=0}^{M-1}\sum_{v=0}^{N-1} F(u,v)\exp\left[i2\pi\left(\frac{mu}{M}+\frac{nv}{N}\right)\right] \tag{15}$$

where: $m = 0,\ 1,\ldots,M-1$, $n = 0,\ 1,\ldots,N-1$. The properties of continuous Fourier transform concerning shifting, rotating and resizing remain the same also for the discrete one. However, the discrete Fourier transform given by (12) is a periodic function and implicitly presumes periodicity of the function $f(m,n)$. This is not the case for the continuous transform obtained by optical methods. Periodicity of discrete Fourier transform manifests itself in equations:

$$F(u,-v) = F(u,N-v),$$

$$F(-u,v) = F(M-u,v), \tag{16}$$

$$F(u,v) = F(aM+u,bN+v) \tag{17}$$

where: a and b are integer numbers. For the same reasons similar equations hold for periodic discrete image function $f(m,n)$

$$f(m,-n) = f(m,N-n),$$

$$f(-m,n) = f(M-m,n), \tag{18}$$

and

$$f(m,n) = f(aM+m, bN+n). \tag{19}$$

Formulae (16) and (17) indicate that discrete Fourier transform is a sum of periodically repeated continuous transforms. This can cause a decrease of image quality connected with phenomenon called aliasing (superposition of continuous transforms). To avoid it, the sampling of the image with finite spatial frequency bandwidth should be done satisfying the Shannon's theorem. This theorem states that spatial frequency of sampling should be at least twice as large as maximum bandwidth of the image.

It is also necessary to center the spatial frequencies coordinates $(u, v) = (0, 0)$ in the matrix **F**, in order to apply it into simulated CGH system. This leads to expression of periodical discrete Fourier transform in new coordinates (u', v') such that

$$u' = u + \frac{M-1}{2}, \tag{20}$$

$$v' = v + \frac{N-1}{2}. \tag{21}$$

When above requirements are fulfilled, the simulated CGH performs discrete integration of function $F(u', v')$ for rings and wedges. Formulae describing this discrete process correspond to continuous integration expressed by formulae (3) and (4) and are given by

$$R_i = \sum_{u'=0}^{M-1} \sum_{v'=0}^{N-1} F^2(u', v')\, \Xi_i(u', v'), \tag{22}$$

$$W_i = \sum_{u'=0}^{M-1} \sum_{v'=0}^{N-1} F^2(u', v')\, \Psi_i(u', v') \tag{23}$$

where functions: $\Xi: \mathbf{R}^2 \to \{0, 1\}$ and $\Psi: \mathbf{R}^2 \to \{0, 1\}$ are defined as

$$\Xi_i(u', v') = \begin{cases} 0 \iff (u', v') \notin \mathrm{RING}_i \\ 1 \iff (u', v') \in \mathrm{RING}_i, \end{cases} \tag{24}$$

$$\Psi_i(u', v') = \begin{cases} 0 \iff (u', v') \notin \mathrm{WEDGE}_i \\ 1 \iff (u', v') \in \mathrm{WEDGE}_i. \end{cases} \tag{25}$$

Outputs from simulated CGH form a feature vector consisting of elements R_i for $i = 1, \ldots, I_r$ and of elements W_i for $i = 1, \ldots, I_w$. The size of the vector is determined by the number of rings and wedges $I = I_r + I_w$. With the above assumptions, the process of feature extraction performed by simulated CGH can be formally described as a function $\zeta: \mathbf{R}^{MN} \to \mathbf{R}^I$, where certainly $MN \gg I$ and the dimensionality reduction $\rho = MN/I$. The feature vector of size I is the input for ANN-based classifier. For this purpose three-layered feed-forward neural network is used.

3. Rough sets in evolutionary optimization of the simulated CGH

The simulated CGH-ANN pattern recognition system described in the previous section can be optimized. The optimization can be done for CGH-based feature extractor and for ANN-based classifier. Since methods for optimization of neural networks are thoroughly described in [15]–[18], in this paper only the problem of the CGH mask optimization is discussed. This method performs stochastic search in the space of possible solutions.

3.1. Objective function

The proper definition of an objective function in optimization of feature extractor is not trivial, since feature extraction is an intermediate stage of the recognition, and expected values of features are unknown. Therefore the quality of features cannot be measured directly by some kind of error function indicating the deviation of actual features from expected ones. However, although expected features are unknown, there is a possibility of measuring the consistence of decision table built on the base of these features and the class to be recognized. The rough set theory introduced by PAWLAK [19] and extended by MRÓZEK [20] to deal with decision tables, is a mathematical formalism that is able to determine such dependences.

CYRAN and MRÓZEK [21] showed that a rough set based coefficient $\gamma_C(D^*)$, called the quality of approximation of classification D^* with respect to indiscernibility relation $I(C)$ generated by the set of decision attributes C, can be used as objective function in the CGH optimization. To apply it, one needs to associate the set of features generated by CGH (set of ring and wedge values R_i and W_i) with the set of conditional attributes C of the decision table. The class to be recognized should be associated with the only element in the set of decision attributes D. Besides, since rough sets are defined for discrete values of conditional attributes, it is necessary to discretize the values of features from CGH.

Let us denote by V_C a domain for attributes from set C. Furthermore, let ξ be the discretization factor such that: $\xi = \mathrm{card}(V_C)$ and $V_C = \{0,\ldots,\xi-1\}$. Then the discretization of features can be expressed as $\Delta: \mathsf{R}^I \to V_C^I$. Certainly, the process of generating by CGH the discretized conditions of decision rule, denoted by $\chi: \mathsf{R}^{MN} \to V_C^I$ is given by

$$\chi = \zeta \circ \Delta. \tag{26}$$

It is easy to see that the discretization factor $\xi = 2$ makes the most restrictive conditions for the function χ to generate a consistent decision table (*i.e.*, such that $\gamma_C(D^*) = 1$).

3.2. Modifications of evolutionary algorithm

Evolutionary algorithms process chromosomes. To apply evolutionary approach to optimization of CGH, besides the definition of objective function (equal to fitness of the chromosome), it is necessary to define the chromosome representation. Obviously, the chromosome has to describe uniquely the CGH. It is evident that for defining

I_r rings $I_r - 1$ genes are required (each gene represents the outer radius of the ring). Similarly, for I_w wedges $I_w - 1$ genes are needed (each gene represents the angle of the second arm of the wedge with horizontal axis). Therefore the structure of CGH (of a constant size) can be uniquely defined by a chromosome with $I_r + I_w - 2$ real-valued elements. However, it should be pointed out that elements of chromosome corresponding to rings must be sorted to define I_r rings. If they are not, the actual number of rings that they define I_{rA} is different from presumed number I_r ($I_{rA} < I_r$). The same can be said about the genes corresponding to wedges.

To obtain sorted genes of rings and wedges the repair algorithm should be applied. The repair algorithms as techniques for handling the constraints in evolutionary algorithms have been described in [22]. The aim of repair algorithm is to convert infeasible solutions into feasible ones. Such a situation can occur after performing genetic operation on chromosomes. Certainly for the above mentioned representation of rings and wedges in a chromosome, the repair algorithm is just a sorting procedure applied separately for genes of rings and for genes of wedges. The above is true if the aim is to obtain optimized CGH with prefixed number of rings and wedges $I = I_r + I_w$. However, such constraints are not obligatory. If sorting is not applied, then evolutionary process searches for the solution with actual number of rings and wedges $I_A = I_{rA} + I_{wA}$, where $I_{rA} \leqslant I_r$, and $I_{wA} \leqslant I_w$. It causes the evolutionary search to be much longer, but can be motivated by looking for a solution with less number of characteristic features. Optimization with sorting only rings or sorting only wedges is also possible.

The dependence of the objective function $\gamma_C(D^*)$ on the discretization factor ξ requires also a slight modification of typical evolutionary algorithm. This modification has to be introducd to resolve the problem when $\gamma_C(D^*) = 1$ for $\xi > 2$. Such a situation means that objective function is unable to grow (since $\gamma_C(D^*) \in [0, 1]$), and at the same time that conditions for the function χ are not the most restricting. Then the search should be continued with the $\xi_{\text{NEW}} = \xi_{\text{OLD}}/2$ [21]. The optimization in pseudo-code is shown below:

```
t ← 1;
ξ ← 2^trunc(log2(card(U)));
while (ξ ⩾ 2) and (t < MaxGenNum) do
    Select;
    Crossover;
    Mutate;
    Repair;
    for i = 1 to card (U) do
            C[i] ← χ(Image_i)
            d[i] ← c_j
    od
    Evaluate (γ_C(D*));
    if γ_C(D*) = 1 then
        ξ ← ξ/2;
    fi
    t ← t+1;
od.
```

In the above code U denotes the set of all images used for optimization of CGH, $C[i]$ denotes discretized conditions and $d[i]$ denotes a decision for Image_i, belonging to class c_j.

4. Experiments

The CGH-based pattern recognition system described can be applied to a wide area of recognition problems where characteristic features are not easy to obtain from geometrical or topological properties of the image. Below, the experiments with two examples of such applications are given.

4.1. Classfier of optical fiber distortions

The classifier of the distortion of optical fiber is the first example. The idea of optical arrangement for this experiment is presented in Fig. 5.

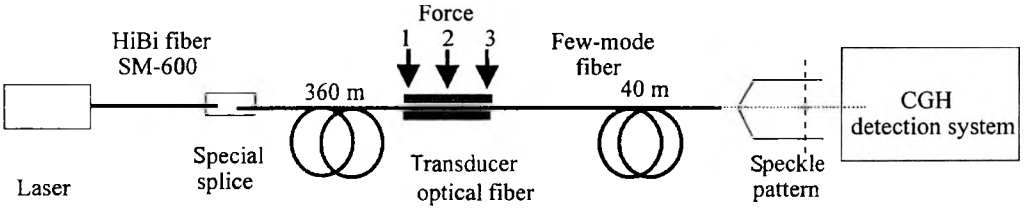

Fig. 5. Optical setup of the optical fiber distortion recognizer [8].

The coherent light passes through a few-mode optical fiber. The distortion of the fiber changes the conditions of inter-modal interference. Therefore, intensity speckle patterns on the output of the fiber are dependent on that distortion. Such images (presented in right upper corners in Fig. 6) are placed in the input plane P1 of the system presented in Fig. 4 or they are input images for software simulation of the system. Figure 6 presents also three-dimensional diagrams of Fourier transform intensities for corresponding speckle images.

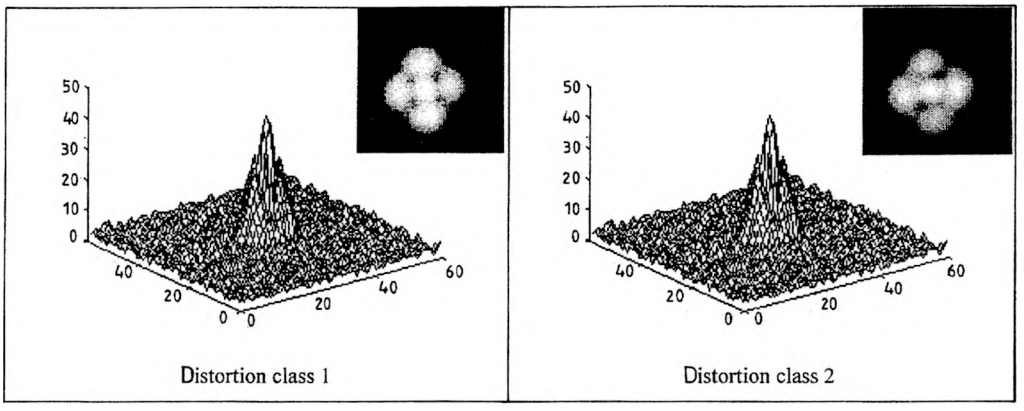

Fig. 6, continued

continued

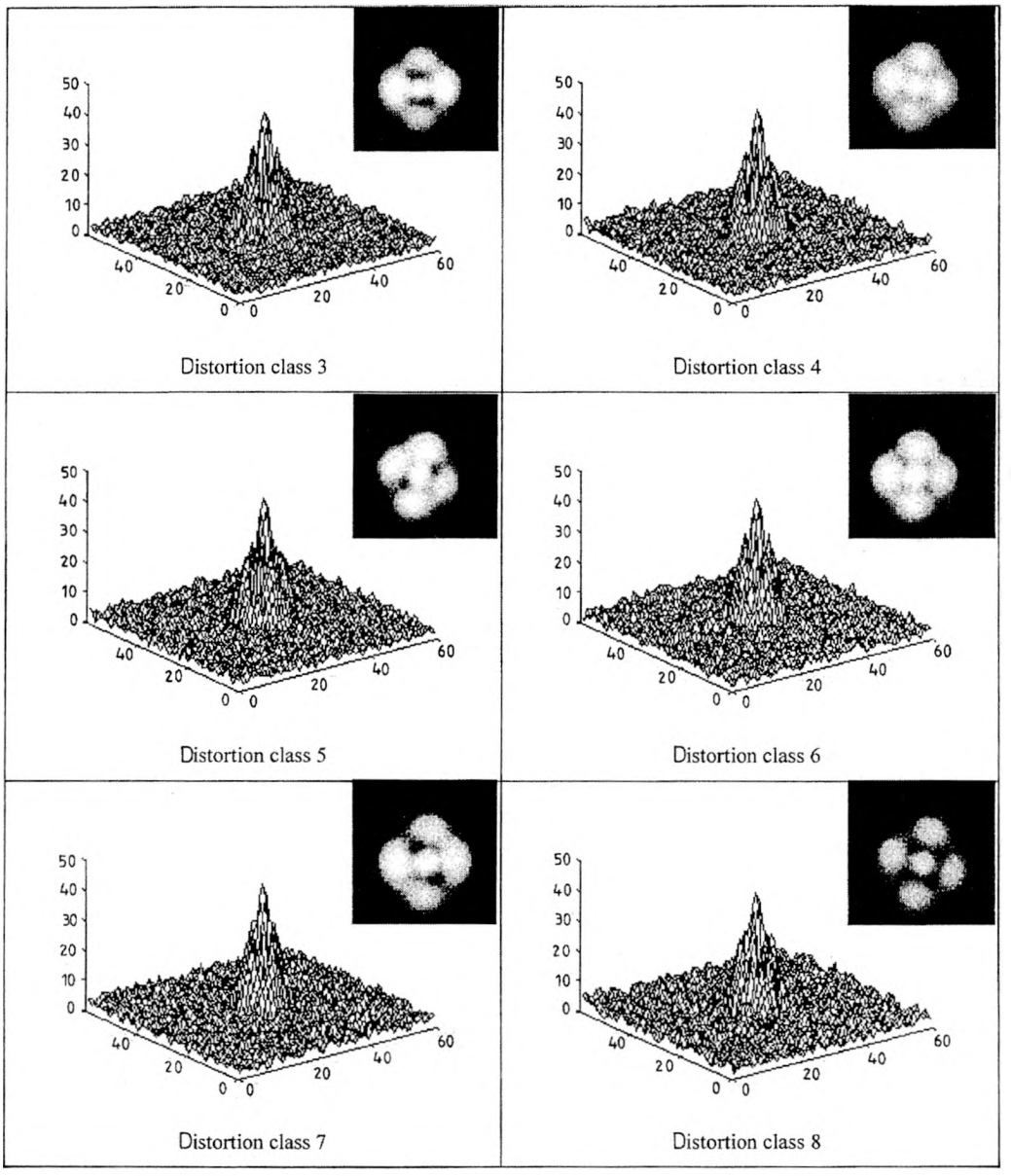

Fig. 6. Input and Fourier images of speckle structures.

The simulated system was optimized with rough-evolutionary algorithm for 128 images belonging to 8 distortion classes. When rings and wedges were sorted, the algorithm found optimal CGH in 29 generation. The mask for optimal CGH in this case is presented in Fig. 7a. If only rings were sorted, the optimal CGH was found in

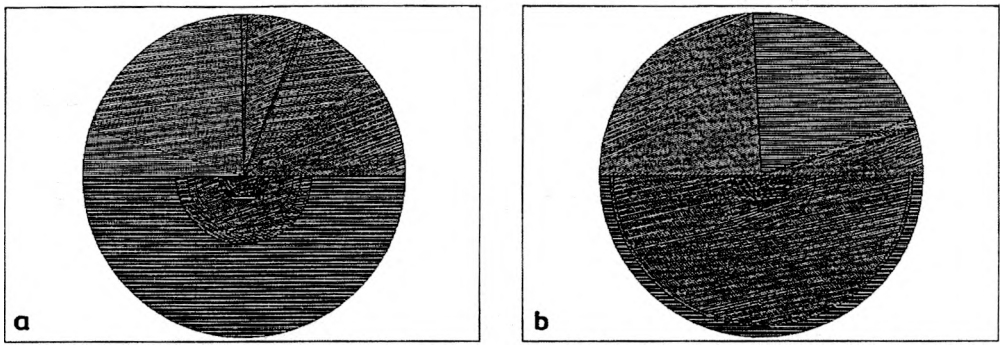

Fig. 7. Optimal CGH masks for 16 features (a) and 13 features (b).

300 generation. This CGH mask is given in Fig. 7b. It can be seen that the evolutionary search was longer without sorting of wedges, however, found optimal CGH performed feature extraction with larger dimensionality reduction $\rho = 315$ (compared to $\rho = 256$ for CGH obtained with the use of full repair algorithm). Both CGHs generated consistent decision table with discretization factor $\xi = 2$.

The optimization proposed was confirmed using the ANN-based classifiers. Classifiers of features extracted by optimal CGH gave answers with normalized decision error (for testing set) ranging from 2.8% to 3.8%. At th same time, classifiers of features extracted by standard CGH answered with the error equal to 4.8% [21].

4.2. Engine and gear condition estimator

The method described in Sections 2 and 3 is universal, thus can be used in solving several problems. The classifier of optical fiber distortion was described earlier; here the description of the automatic system for estimation of engine and gear condition is given. This is the most important problem that appears during its lifetime. There are many methods of performing this task. Some of them are based on analysis of rub products gathered in lubricating oil. These methods use a dependence of engine condition on quantity and kind of products. Two of them recognize these parameters by analyzing radiation of excited atoms. These are X-ray fluorescence spectrometry (XRF) method and atomic emission spectrometry (AES) method. Both of them are very accurate, but also complicated, because they require special measuring devices and staff. WOLSKI [23] proposed another method based on comparison of microscope pictures of sample oil with prepared pattern collection. This pattern collection must contain a set of characteristic pictures for each device being tested. In the mthod, before comparison samples are put into magnetic field for initial sorting of ferromagnetic particles. Thus this method is called ferrographic. The method presented below is based on it. However, contrary to classical ferrographic method, it requires minimum human activity during measuring process.

A scheme of measuring system is shown in Fig. 8. An image of oil sample placed into electromagnet is transferred to CCD camera by optical fiber (fiberscope).

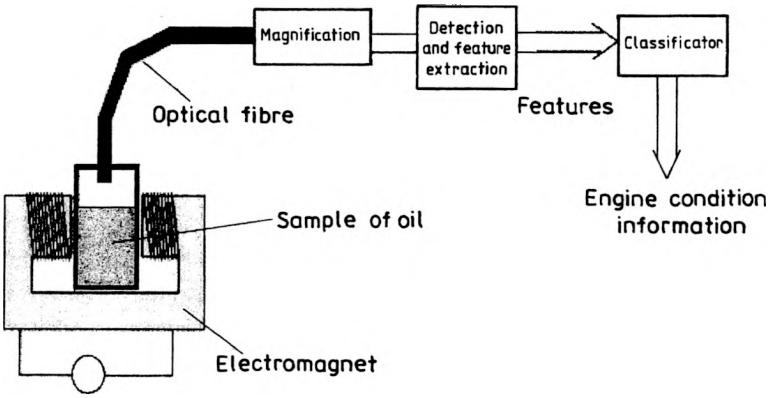

Fig. 8. Scheme of measuring system [24].

During this operation, image magnification is also needed because the diameter of the region of interest is usually less than 400 μm.

Although image from CCD camera contains sufficient information for proper classification, it must be preprocessed to extract interesting features and decrease the number of data transmitted into classifier. Those functions are realized by

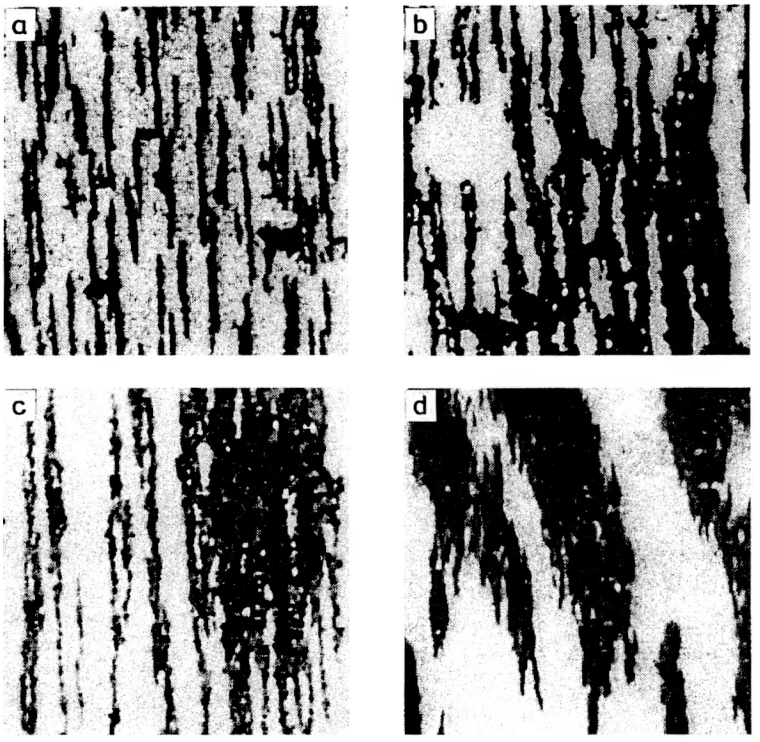

Fig. 9. Examples of engine gear images for each group of wear: normal (a), increased (b), intensive (c) and corrosive (d).

optimized CGH-based pattern recognition system described above. Then features obtained in this step are used in classifier to determine actual condition of an engine (or gear). In the experiment, images of lubricating oil of engine bearing and gear have been used. All source images are of size 600×400 μm. Since resolution is not critical, each image is taken at 600×400 pixels size and then truncated into square region and resized into 256×256 pixels in order to optimize discrete fast Fourier transformation (FFT) operation. All images are split into four classes: normal, increased, intensive and corrosive wear. The dependence between images and classes is determined by the amount of products gathered in oil. The greater elements are more important because the fact of their amount being increased is caused by more serious wear.

Pictures shown in Fig. 9 present examples of each of the above classes taken from the gear. Picture **a** represents normal wear. There are many small ferromagnetic wear products and rare greater elements. Picture **b** presents image of increased wear. It contains several products of larger diameter (size 30×20 μm) and many small products lying along magnetic field lines. Next image (c) is an example of intensive wear containing many large (20×60 μm in size) products and several small products. The last picture (**d**) presents an image of corrosive wear with rust gathered in lubricating oil that indicates considerable waste.

Every image was prepared for feature extraction in several steps. First, each picture was truncated and scaled into 256×256 points. This operation reduced picture size (and, of course, the amount of data) without significant loss of information. Pictures presented in Fig. 9 had to be brightened because most of them were dark. This was done only for illumination purposes. Next, the noise was removed from pictures using a simple smoothing filter that can be presented as a matrix

$$M = \frac{1}{9}\begin{bmatrix} 1 & 1 & 1 \\ 1 & 1 & 1 \\ 1 & 1 & 1 \end{bmatrix}. \tag{27}$$

Theoretically, matrix of a greater size could also be used but then the loss of information would be too serious. After smoothing, images were processed by discrete FFT to obtain data for simulated CGH-based system.

Pictures shown in Fig. 10 present images in frequency domain (after discrete FFT) with drawn rings and wedges, whereas proportions between intensities of rings and wedges are shown in Fig. 11. The data shown in Fig. 11 contain values of R_i and W_i calculated relatively to $\max(R_i)$ and $\max(W_i)$, respectively.

It follows from the data presented that normal wear images contain more diffused power spectrum. This also results in more power in higher rings (R_4, R_5, *etc.*). Many small products gathered in oil and appearing in images cause this. On the contrary, intensive and corrosive wear images contain power mainly in lower rings (closer to DC component). Images in these cases contain many large products. Moreover,

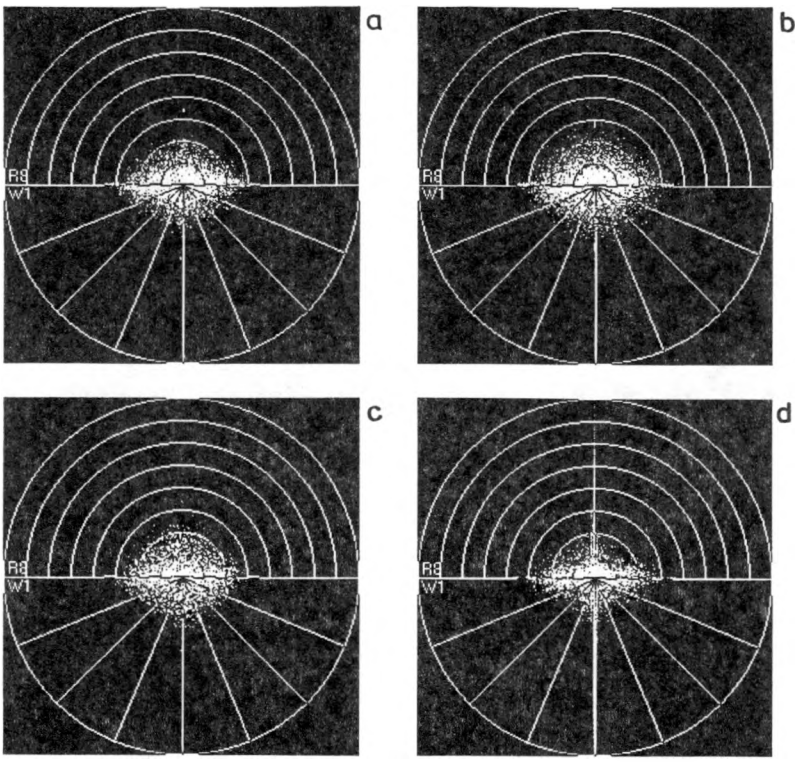

Fig. 10. Image from Fig. 9 (**a** — normal, **b** — increased, **c** — intensive, **d** — corrosive wear) after processing.

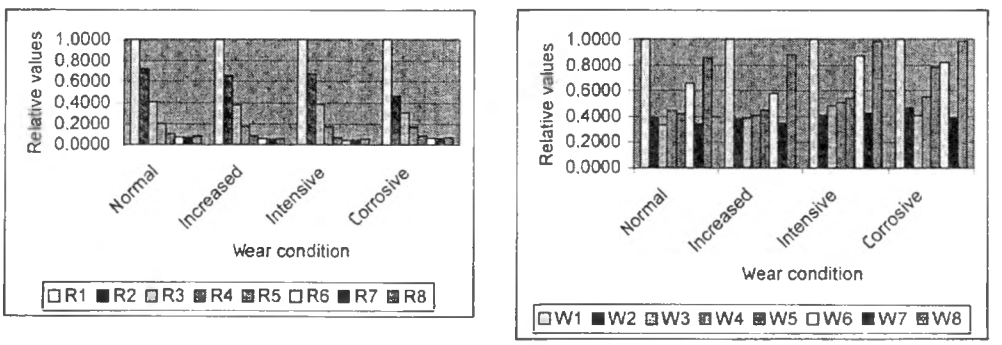

Fig. 11. Relative power of rings and wedges drawn in Fig. 10.

analyzing graphs presented in Fig. 11, one can notice that for classification purposes the dependence between wedges is not so good as between rings. Data preprocessed in such a way can be used for the above presented evolutionary optimization of CGH mask to obtain automatic optimal CGH-based recognizer of gear (or engine) condition.

5. Summary and conclusions

The theory of optimized pattern recognizer based on computer-generated hologram and artificial neural networks has been presented in this paper. The CGH was used as a feature extractor of frequency domain images (continuous and discrete), whereas neural network classified features obtained from CGH. The original rough-set evolutionary optimization of simulated CGH was also given. The modifications of typical evolutionary algorithm caused by requirements of rough set based objective function were explained and modified algorithm was supplied. Also, the need of applying the repair algorithm to deal with the constraints concerning the structure of genes (sorted, unsorted) was discussed.

The theoretical investigations presented have many practical applications in a wide range of problems connected with automatic recognition and classification of images in technical science and medicine. Two examples of an application of optimized recognizer have been presented. The first was classifier of optical distortion. The experimental results confirmed good overall quality of the system (normalized decision error less than 3%), as well as a decrease of this error after optimization (from 4.8% to 2.8%). The usage of restricting repair algorithm (applied to rings and wedges) caused optimization to be very fast. When this algorithm was not applied to genes corresponding to wedges, the evolutionary search was longer, however the optimized simulated CGH extracted features with greater dimensionality reduction $\rho = 315$ (compared to $\rho = 256$) since the number of wedges had been reduced during optimization. Possible applications of such a classifier include automatic recognizers of distortion in flying airplanes (with optical fiber placed in wings) or controlling the traffic (with optical fiber placed across the road).

The second experiment concerned automatic estimation of engine condition on the basis of lubricating oil images. The initial results presented in the paper are very promising. There are considerable dependences between power spectrum after discrete FFT and condition of the device being tested. This suggests that the transformation proposed provides for proper extraction of features. But, of course, there can be better way of obtaining similar results. First observation suggests to remove electromagnet. This part was necessary only for recognition made by human to decrease the region containing interesting particles. After that the power spectrum would be more uniform (in all directions). The second observation is that in order to increase correctness of classification many images from several regions must be taken during measuring process. This work is still continued and further research is needed before presenting more detailed results (decision errors, comparison with other methods, *etc.*).

Acknowledgements — The authors would like to acknowledge the Polish State Committee for Scientific Research (KBN) for funding this program under MUT statutory activity PBS-170 and grant No. 0 T00A 021 17.

References

[1] GEORGE N., WANG S., VENABLE D. L., Proc. SPIE **1134** (1989), 96.
[2] MARSHALL M., BENNER R., Opt. Engin. **31** (1992), 947.
[3] JAROSZEWICZ L. R., MERTA L, KIEŻUN A., Proc. SPIE **3555** (1998), 337.
[4] GEORGE N., WANG S., Appl. Opt. **33** (1994), 3127.
[5] CASASENT D., SONG J., Proc. SPIE **523** (1985), 227.
[6] SAXENA L, HORAN P. G., *Optical implementation*, [In] *Handbook of Neural Computation*, [Eds.] Fiesler E., Baele R., Chapt. F1.2, F1.2:1–F1.2:8. Institute of Physics Publishing and Oxford University Press, New York 1997.
[7] CYRAN K. A., MRÓZEK A., *Hybrid methods in pattern recognition*, Proc. of VIII Workshop on Intelligent Information Systems, Ustroń, Poland 1999, 12–16.
[8] JAROSZEWICZ L. R., CYRAN K. A., KŁOSOWICZ S. J., MRÓZEK A., Proc. SPIE **3744** (1999), 386.
[9] CYRAN K. A., Proc. SPIE **3744** (1999), 241.
[10] PARKER J. R., *Practical Computer Vision Usimg C*, Wiley Inc., New York 1994.
[11] SCHALKOFF R., *Pattern Recognition — Statistical, Structural and Neural Approaches*, Chap. 10–12, Wiley Inc., Singapore 1992.
[12] MERTA L, JAROSZEWICZ L. R., KIEŻUN A., Opt. Appl. **29** (1999), 171.
[13] POTTER D., *Computational Methods of Physics — Computer Physics*, (in Polish), PWN, Warszawa 1982.
[14] SONKA M., HLAVAC V., BOYLE R., *Image Processing and Machine Vision*, Chap. 10, Chapman & Hall, Cambridge 1993.
[15] TADEUSIEWICZ R., *Neural Networks* (in Polish), Akademicka Oficyna Wydawnicza RM, Warszawa 1993.
[16] ŻURADA J., BARSKI M., JĘDRUCH W., *Artificial Neural Networks* (in Polish), Wydawnictwo Naukowe PWN, Warszwa 1996.
[17] CIEMNIEWSKI Z., LETKIEWICZ S., CYRAN K. A., *Connectionist approach in diagnosis support systems on the basis of feed-forward ANN giving prognosis in urology and cardiology*, Proc. Internat. Workshop: *Biomedical Engineering and Medical Informatics*, Gliwice, Poland, 1997, 100–104.
[18] CYRAN K. A., LETKIEWICZ S., WOJCIECHOWSKI P., KOŁOCZEK D., *Use of neural network to recovery prognosis for patients with renal cancer* (in Polish), Zeszyty Naukowe Politechniki Śląskiej, **1337** (1997), 185.
[19] PAWLAK Z., Int. J. Infor. Computer Sci. **11** (1982), 341.
[20] MRÓZEK A., Inter. J. Man-Machine Studies **36** (1992), 127.
[21] CYRAN K. A., MRÓZEK A., Inter. J. Intelligent Systems, (2000), in print.
[22] MICHALEWICZ Z., *Evolutionary computation models — constraint-handling techniques*, [In] *Handbook of Evolutionary Computation*, [Eds.] T. Bäck, D. B. Fogel, Z. Michalewicz, Chapt. C.5, pp. C5.1:1–C5.5:6. Institute of Physics Publishing and Oxford University Press, New York 1997.
[23] WOLSKI J., *et al.*, Report of research works of grant no. 14877/C-T00/95", ITWL — internal elaborate, Warszawa 1996.
[24] JAROSZEWICZ, L. R., PODESZWA T., MRÓZEK A., WOLSKI J., *Idea and first results of fiber-optic sensor for engine estimation condition*, Proc. SPIE (in print).

Received May 22, 1999